MOSAICS: Multiplexed Optimal Signal Acquisition Involving Compressed Sensing

J V Satyanarayana
Department of Electrical Engineering,
Indian Institute of Science
Bangalore, 560012, India,
Email: jvsat29@yahoo.co.in

A G Ramakrishnan
Department of Electrical Engineering,
Indian Institute of Science
Bangalore, 560012, India,
Email: ramkiag@ee.iisc.ernet.in

***Abstract*—It is possible to sample signals at sub-Nyquist rate and still be able to reconstruct them with reasonable accuracy provided they exhibit local Fourier sparsity. Underdetermined systems of equations, which arise out of undersampling, have been solved to yield sparse solutions using compressed sensing algorithms. In this paper, we propose a framework for real time sampling of multiple analog channels with a single A/D converter achieving higher effective sampling rate. Signal reconstruction from noisy measurements on two different synthetic signals has been presented. A scheme of implementing the algorithm in hardware has also been suggested.**

***Index Terms*—A/D Conversion, Nyquist sampling theorem, Bandlimited signals, Fourier sparsity, Real time, Data acquisition, Compressed Sensing, Monopulse radar**

I. INTRODUCTION

THE number of continuous time (CT) signals sampled during operation of the modern industrial, process control, biomedical and avionics equipment has increased by several orders owing to the ever increasing system complexity. A large number of analog to digital converters (ADCs), with moderate to high sampling rates governed by the Nyquist criterion are being included in system designs to cater for the increasing sophistication. The problem can be considerably alleviated by reducing the signal sampling rate if information redundancy under a Nyquist sampling scheme can be exploited provided the signal is known to be sparse in a transformed space, say the frequency domain. Recovery of multi band signals, when a priori knowledge of the band locations and their widths is available, was studied by Landau [1]. Landau identified a minimum required rate equal to the sum of the bandwidths, to achieve perfect reconstruction, under an arbitrary sampling scheme. Sub-Nyquist rate uniform sampling was proposed in [2] for truly bandpass signals. Periodic non-uniform, sub-Nyquist sampling, was studied in [3] and extended for the case of multiband signals in [4]. Signal recovery with only partial knowledge of the spectrum in the presence of mathematical constraints on the band locations, was addressed in [5]–[7]. Periodic, non-uniform, multicoset sampling followed by reconstruction of the signal, achieving Landau sampling rate in the limit has been studied in [8]. Significant contribution towards blind recovery, under a multicoset sampling strategy in a compressed sensing framework, where only the number and widths of the bands are known, has been proposed by Moshali and Eldar [9]. Commendable work on the theory, algorithms, performance bounds and hardware design of an analog to information converter based on random demodulation for sampling a high frequency CT signal using a low rate ADC has been presented in [10]. An innovative scheme using a multiplexer to facilitate random sampling has been proposed in [11].

The possibility of acquiring multiple signals, sparse on same basis like Fourier, at a reduced sampling rate, using lesser number of ADCs needs to be explored. The focus of our work is towards evolving a hardware architecture, which can employ any arbitrary undersampling scheme, to acquire multiple analog signals, using lesser number of ADCs sampling data at a uniform rate. Reduction in the number of ADCs used to sample IF signals in radar signal processing has a tremendous impact with respect to cost, compactness and power requirement. Further, we desire that the proposed design should support an embedded real time data acquisition system, with streaming input data. We call the proposed scheme as 'Multiplexed Optimal Signal Acquisition Involving Compressed Sensing' for reasons which will be obvious in Section IV, and hereafter refer to it as MOSAICS.

II. CHARACTERISTICS OF SIGNAL

Consider a class $\mathcal{S}$ of CT real signals such that a signal $S \in \mathcal{S}$, if S as a function of time comprise segments s_k, such that

$$S(t) = s_k(t) \text{ for } t_{k-1} \leq t \leq t_k \text{ and } k = 1,2,\dots,\infty. \quad (1)$$

Also, $L = inf\{l_k \in \mathbb{R} : l_k = t_k - t_{k-1}, \forall k = 1,2,\dots,\infty\}$ is known a priori and each s_k is such that it has at most $K \ll l_k R_{NYQ}$ frequency components with frequencies less than R_{BW}, the bandwidth of the signal and $R_{NYQ} = 2R_{BW}$ is the Nyquist sampling frequency. In other words, the signal is a concatenation of band limited 'Locally Fourier Sparse' (LFS) segments, the duration of which has a lower bound L that is known a priori. Within any segment, the Fourier spectrum of the signal remains unchanged. Broader signal classes can be approximated over short time intervals to the discrete multitone signals within $\mathcal{S}$ by means of windowing [10].

III. SPARSE RECOVERY

Consider a vector $\boldsymbol{\xi} \in \mathbb{R}^{\boldsymbol{\eta}\times\mathbf{1}}$obtained by sampling any LFS segment s_k in the time interval $[\tau_1, \tau_2]$ where $t_{k-1} \leq \tau_1$, $\tau_2 \leq t_k$, at the Nyquist time instants τ_1, $\tau_1 + t_{NYQ}$, $\tau_1 + 2t_{NYQ}$, … $\tau_1 + (\eta - 1)t_{NYQ}$ where $t_{NYQ} = 1/R_{NYQ}$. We refer to such a section of duration $\tau_2 - \tau_1$ in an LFS segment as a reconstruction segment (RS). Each LFS segment comprises one or more RSs. Suppose we measure the signal at only $\theta < \eta$, Nyquist time instants in the RS, and are still able to reconstruct the signal, then lesser number of A/D conversions would be required. Let the measurement process be represented by the measurement matrix $\boldsymbol{\phi} \in \mathbb{R}^{\theta\times\eta}$ consisting of θ randomly chosen rows of the identity matrix $I \in \mathbb{R}^{\eta\times\eta}$. The measurement vector, $\boldsymbol{f} \in \mathbb{R}^{\theta\times 1}$ is given by

$$\boldsymbol{f} = \boldsymbol{\phi\xi} \tag{2}$$

Let $F^{-1} \in \mathbb{C}^{\eta\times\eta}$ be the inverse discrete Fourier transform (IDFT) matrix. We wish to find a vector $\boldsymbol{g} \in \mathbb{C}^{\eta\times 1}$ which satisfies

$$\boldsymbol{\phi}F^{-1}\boldsymbol{g} = \boldsymbol{f} \tag{3}$$

Assuming (3) is solvable, we can get back the reconstruction segment as $\boldsymbol{\xi} = F^{-1}\boldsymbol{g}$. The crux of the problem lies in solving (3) in which the number θ of equations, is less than the number η of unknowns. Therefore, the solution set is not unique. The hope exists in the fact that $\boldsymbol{g}$ is sparse, as $K \ll \eta$, which is based on one of the tenets in the signal model. A recent paradigm in the field of data acquisition known as compressed sensing (CS) [12]-[13] has promulgated the idea that it is possible to obtain a solution to the undetermined set of equations, provided that the solution is sparse. Under a CS framework [14], (3) can be solved as

$$\boldsymbol{g} = arg\ min\|\boldsymbol{h}\|_{\mathbf{1}} \text{ subject to } \boldsymbol{\phi}F^{-1}\boldsymbol{h} = \boldsymbol{f} \tag{4}$$

$$\text{followed by } \hat{\boldsymbol{\xi}} = F^{-1}\boldsymbol{g} \tag{5}$$

We accommodate for ADC measurement noise, by altering the constraint in (4) as,

$$\mathrm{M}(\boldsymbol{\phi}F^{-1}\boldsymbol{h} - \boldsymbol{f}) < \epsilon \tag{6}$$

where, M is defined as, $M(v) = \|v\|_2 / \sqrt{N} \quad \forall v \in \mathbb{R}^{N\times 1}$ and ϵ is the upper bound on the rms noise. Let $SMNR = 20log\left(\frac{\mathrm{M}(\boldsymbol{f})}{\epsilon}\right)$, be the signal-to-measurement noise ratio in dB. Therefore, ϵ is calculated as

$$\epsilon = \frac{\mathrm{M}(\boldsymbol{f})}{10^{\left(\frac{SMNR}{20}\right)}} \tag{7}$$

Since the measurement matrix is the trivial downsized identity matrix, no elaborate measurement setup is required for projecting the signal on a basis incoherent [15] with the DFT matrix. The measurement vector is formed by just skipping the measurements at $\eta - \theta$ timing instants. It has been proved in [16] that the l_1 norm being convex, (4) to (6) can be solved as a convex optimization problem in polynomial time.

A. Overlapped reconstruction segments

The signal is acquired and reconstructed as a series of overlapping RSs. Thus most of the elements of the vector $\boldsymbol{f}$, can be obtained from the preceding RS that has been already reconstructed, while the remaining are obtained by directly measuring the signal at randomly spaced time instants. Let j denote the RS which contains the boundary between two LFS segments. Then, the boundary can be detected easily since

$$\left\|\boldsymbol{g}_j - \boldsymbol{g}_{j-1}\right\|_2 > \delta \tag{8}$$

where δ is a small threshold. The RS immediately following an LFS boundary employs samples from direct measurement on the signal, that is, without any overlap with the previous RS. Overlap continues to be there for the subsequent RSs until another boundary is detected. The extent of overlap between successive RSs depends on the desired accuracy of detecting the boundary between two LFS segments. Given an overlap of ψ samples, the boundary is located within an accuracy of $\eta - \psi$ samples.

IV. MULTIPLEXED SIGNAL ACQUISITION

With only $\theta < \eta$ measurements being done in an RS on a single channel, the remaining $\eta - \theta$ Nyquist sampling instants can be used for multiplexed acquisition of other analog channels. This is at the crux of the operation of MOSAICS in which no sampling time instant is left unutilized. Hereafter we use the prefix/suffix i, wherever required, to identify individual analog channels.

A. Algorithm specifications

The following a priori information about each analog channel acquired in MOSAICS is provided as input to the algorithm:

- Highest frequency, R_{BW}^i, $i = 1 \ldots \mathcal{N}$ across all LFS segments for each channel in the total duration of the acquisition. $\mathcal{N}$ is the number of analog channels.
- Frequency sparsity, K_i – maximum number of non-zero frequency components in the signal.
- Minimum duration of an LFS segment, L_i – given in time units, this is required to fix η_i, the length of RS.
- Accuracy of boundary detection, ε_i – specified in time units, this input decides the extent of overlap between consecutive RSs of the signal.
- Signal-to-measurement noise ratio, $SMNR_i$

B. Algorithm execution

The system in Fig. 1 consists of two blocks - the acquisition block (AB) and the reconstruction block (RB), which operate in parallel. The AB consists of a single channel ADC sampling data at a uniform rate R_{OP}, the operating frequency of MOSAICS equal to twice the maximum bandwidth of all the channels.

$$R_{OP} = 2\left(max\left\{R_{BW}^i, i = 1..\mathcal{N}\right\}\right) \tag{9}$$

R_{OP} is generated by the clock in the system. The operation of the system consists of a series of contiguous acquisition cycles, with β samples being acquired in each cycle. At the start of each acquisition cycle, the sampling pattern (SP) generator generates a pattern ρ, allocating at random the β sampling instants to the $\mathcal{N}$ channels like in a mosaic. This ensures that the sampling of the channels is randomly interspersed throughout the acquisition which is required for successful reconstruction [17]. The number of slots in the acquisition cycle that are allocated to each channel depends on the desired level of reconstruction accuracy and the Fourier sparsity. At each clock tick, the SP generator outputs the next element in the sampling pattern which, after being coded as binary, is fed to the analog multiplexer selection lines. The multiplexer, also driven by the clock, selects the chosen channel, which is then sampled by the ADC. Though, the ADC operates at a uniform sampling rate the sampling of the

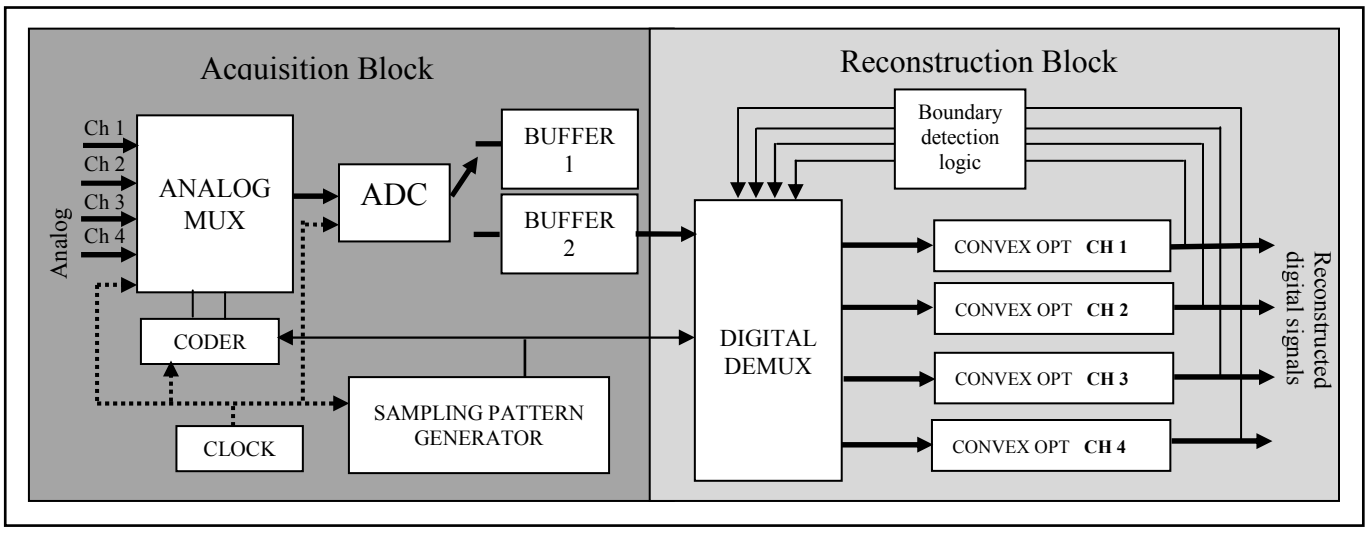

Fig. 1 Multiplexed Optimal Signal Acquisition involving Compressed Sensing

individual channels is non-uniform. At the end of each acquisition cycle (AC), there is a software controlled buffer swap. RB operates on the data in the inactive buffer acquired in the previous cycle, while AB writes newly acquired samples into the active buffer. Given the sampling pattern for each acquisition cycle, the digital demultiplexer (DD) block segregates the samples in the inactive buffer into the separate channels. The DD block forms the vector $\boldsymbol{f_i}$, $i = 1 \ldots \mathcal{N}$ for each channel with the help of a window pointer followed by multiplication of the elements of $\boldsymbol{f_i}$ with the appropriate elements of a Kaiser window of size η_i. At the end of each acquisition cycle, the DD block checks for every channel, if the reconstruction window of the channel is completed by comparing the corresponding window pointer with η_i, the chosen size of the RS for the channel i. If so, then the vectors $\boldsymbol{f_i}$ are released to the $\mathcal{N}$ convex optimization (4)-(6) blocks for each channel based on interior point methods. De-windowing is done by dividing each element of $\hat{\xi}$ in (5), by elements of the window. The process of forming the vector $\boldsymbol{f_i}$ for a channel may span more than one AC, depending on the chosen size of the RS for the channel. Consequently, the reconstruction of segments for different channels may not be synchronized. The result of the boundary detection logic (8) including decision on whether there should be an overlap with the preceding RS is fed back to the DD block. Finally, all the necessary initializations for the next AC are done.

C. Parameters affecting performance

In this section, we focus on several parameters which affect the performance of MOSAICS.

Effective sampling rate

With $\mathcal{N}$ channels being acquired simultaneously, the effective sampling rate of MOSAICS is

$$R_{EFF} = \mathcal{N} R_{OP} \tag{10}$$

For faithful reconstruction of all channels in a conventional setup with dedicated ADCs, the required rate is

$$R_{NYQ} = 2 \sum_{i=1}^{\mathcal{N}} R_{BW}^{i} \tag{11}$$

The advantage gained in MOSAICS is significant if the utilization factor we define as

$$UF = \frac{R_{NYQ}}{R_{EFF}} \times 100 \tag{12}$$

is above 90 percent so that there is no oversampling for any channel. This is true if R_{BW}^{i}, $i = 1 \ldots \mathcal{N}$ have values close to each other. This can be made possible, since while designing a complete data acquisition system based on multiple MOSAICS blocks, the analog channels can be clustered into groups comprising channels with nearby bandwidths. Each group can be handled by a separate MOSAICS block.

Length of reconstructed segment

Given L_i, as input to the algorithm, the length η_i of RS for each channel is chosen to be the largest integer multiple of the ADC buffer size, β that is smaller than $L_i R_{OP}$. This is done to ensure that a boundary is not missed.

$$\eta_i = ceil\left(\left(\frac{L_i R_{OP}}{\beta}\right) - 1\right)\beta \tag{13}$$

where, $ceil(\varrho) = smallest\ n \in \mathbb{Z}, such\ that\ n \geq \varrho$. By choosing η_i to be a multiple of β, it is ensured that the completion of the reconstruction window is always synchronized in real time with the end of acquisition cycles.

Number of measurements in each RS

It has been proven in CS theory [13], that the RS can be faithfully reconstructed with a probability of almost 1, if

$$\theta_i \geq ceil\left(CK_i' log(\eta_i / K_i')\right) \tag{14}$$

where $K_i' = 2K_i$ and K_i is the frequency sparsity, a specification to the algorithm. The factor of 2 takes care of the mirror image in the DFT spectrum for real signals. Our choice of a value of 5 for the constant C is based on [18]. In the RS that immediately follows an LFS boundary, as explained in the previous section, all the samples have to be taken by direct measurements on the signal, from $\gamma_i = \eta_i / \beta$ acquisition cycles. To acquire θ samples from γ cycles, within each cycle, $\tau_i = \theta_i / \gamma_i$ measurements of channel i are required. In the worst case, it may so happen that the LFS boundaries of the $\mathcal{N}$ analog channels are detected after the same acquisition cycle, in which case for feasible reconstruction

$$\sum_{c=1}^{\mathcal{N}} \tau_c \leq \beta \tag{15}$$

Ideally, the equality sign should hold, so that all the Nyquist time instants in the acquisition cycle are utilized. However, if

TABLE 1
FREQUENCY CHARACTERISTICS OF THE SIGNAL FOR TEST INPUT 1

CHANNEL 1		CHANNEL 2		CHANNEL 3		CHANNEL 4	
Time in ms	Freq. in kHz	Time in ms	Freq. in kHz	Time in ms	Freq. in kHz	Time in ms	Freq. in kHz
0 - 23.5	7.2, 8.4, 3.8	0 - 26.1	4.5, 5.1, 6.3	0- 18.5	5.4, 8.1, 9.3	0 - 32.5	3.6, 6.0, 2.4
23.5 - 45.3	1.8, 2.3 , 7.4	26.1 – 39.6	1.2, 3.5, 8.3	18.5 – 41.8	1.8, 4.2, 7.5	32.5 – 47.8	5.9, 7.1, 8.0
45.3 – 61.2	5.9, 8.1	39.6 – 53.2	6.4, 9.7	41.8 – 58.2	8.6, 9.3	47.8 – 65.6	2.3, 1.7, 3.2
61.2 - 78.2	3.9, 7.5, 8.2	53.2 – 76.5	5.3, 8.8, 9.1	58.2 – 75.2	2.5, 7.8, 9.1	65.6 – 78.7	3.5, 7.2
>78.2	5.6, 6.1, 9.3	>76.5	1.6, 3.3, 7.5	>75.2	3.3, 6.6	> 78.7	1.8, 3.1, 4.3

this is not so, it is possible to regroup the analog channels in the system into different MOSAICS blocks so as to ensure that (15), preferably as equality, holds within each block.

Buffer size

The peak computation time t_{RB}^{peak} of RB is required in the cycle in which all the $\mathcal{N}$ channels have to be reconstructed, through convex optimization, due to coincident completion of the respective reconstruction windows. To cater for this worst case situation each acquisition cycle should be of duration t_{RB}^{peak} and therefore the size β of the buffers 1 and 2 can be

$$\beta = t_{RB}^{peak} R_{OP} \tag{16}$$

t_{RB}^{peak} depends on a number of factors like - the number of analog channels, $\mathcal{N}$, the size η_i of the RS, for each channel and the speed of the host processor can be easily estimated beforehand. A large t_{RB}^{peak} due to the above factors does not alter R_{EFF} in (10) and results only in a time lag, between the reconstructed outputs of MOSAICS and the original signals. The extent, to which this lag can be tolerated, is in turn governed by the demands of the end application.

V. IMPLEMENTATION IN HARDWARE

The hardware design for MOSAICS, shown in Fig. 2, consists of a single channel ADC and an analog multiplexer. The digital demultiplexer, the convex optimization blocks, the sampling pattern generator and the boundary detection logic can be implemented in software running on the processor. Based on the generated sampling pattern, the channel selection input is given to the analog multiplexer through the address bus of the host processor. Many commercially available ADCs have a built in multiplexer. The buffers 1 and 2 exist in the RAM. The DMA is initialized by the processor to perform a direct memory transfer from the ADC to the RAM. If multiple MOSAICS blocks exist in a system, then they can share a common processor, RAM and DMA.

VI. SIMULATIONS AND RESULTS

A. Test signal 1

Four CT signals are acquired for a duration of 100 msec.The time-frequency characteristics of four channels of the test input are shown in Table 1. $R_{OP} = 20\,kHz$ and $R_{EFF} = 80\,kHz$. To simulate measurement noise, white Gaussian noise at an SNR of 20 dB is added to each measured sample in the buffer at the end of every acquisition cycle using the Matlab function *awgn*. In a snapshot of the reconstructed signals in the interval: 35 - 50 ms, shown in Fig. 3, the reconstruction (red) has an excellent match with the original signal (black). Consistent with the time frequency characteristics, the reconstruction slightly deviates from the original signal around LFS boundaries, at: 45.3 ms for channel 1, 39.6 ms for channel 2, 41.8 ms for channel 3 and 47.8 ms for channel 4. Quantitative measure of the deviation, expressed using PSNR (peak signal to noise ratio) is

$$PSNR(v_1, v_2) = 20log\left[\frac{max(v_1)}{\mathrm{M}(v_2 - v_1)}\right] \tag{17}$$

where $\mathrm{M}(v)$ is as defined before, are given below Fig. 3.

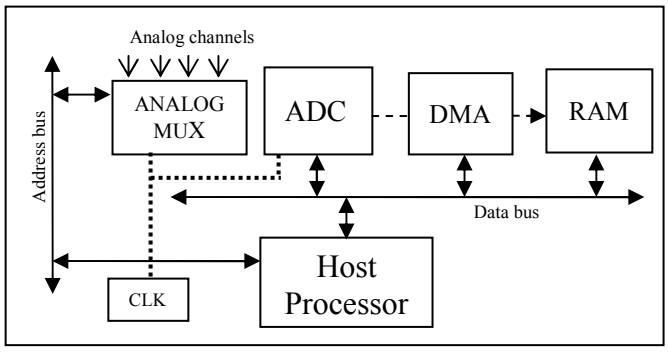

Fig. 2 Hardware design for MOSAICS

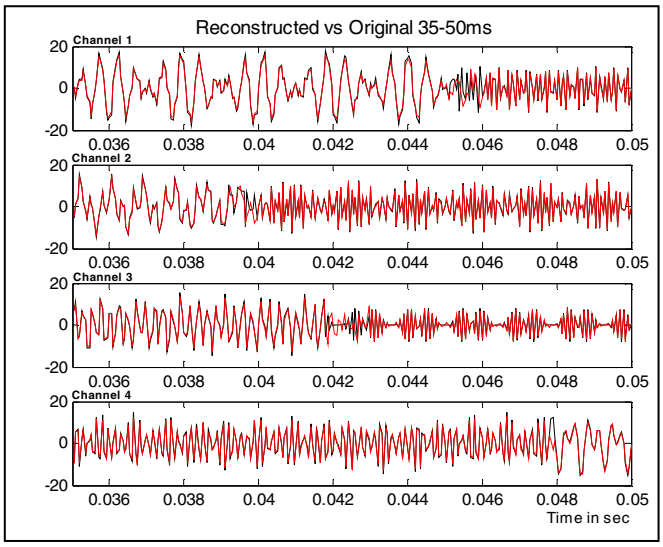

Fig. 3 Reconstructed signal (red) over the original signal (black) for four channels. The PSNR deviations for the channels are channel 1:21.8 dB, channel 2: 25.7 dB, channel 3: 21.4 dB, channel 4: 22 dB

B. Test signal 2

The input of a monopulse radar system [19]–[20], comprises three bandpass RF signals: sum, difference–azimuth and difference-elevation, which are mixed down to IF in 10-100 MHz range. Table 2A gives the time-frequency characteristics for the three IF channels. The frequencies reside in the bands $R_{BW}^{i} = 5\,MHz$ for $i = 1,2,3$. Therefore, under a bandpass

TABLE 2A
FREQUENCY CHARACTERISTIC FOR TEST INPUT 2

CHANNEL 1		CHANNEL 2		CHANNEL 3	
Time μs	Freq. MHz	Time μs	Freq. MHz	Time μs	Freq. MHz
0 – 60	30.5	0 – 70	21.5	0 - 190	41
60 - 110	31.4	70 – 124	23.6	190 – 230	44.1
110 - 160	32.3	124 - 201	21.2	230 - 280	43.5
160 – 230	33.4	201 – 270	24.1	280 – 320	42.2
>230	31.2	>270	22.8	>320	40.5

TABLE 2B
MOSAICS OUTPUT – HIGHEST FREQUENCY COMPONENT

CHANNEL 1		CHANNEL 2		CHANNEL 3	
Time μs	Freq. MHz	Time μs	Freq. MHz	Time μs	Freq. MHz
0 – 60	0.5	0 – 70	1.5	0 - 190	1
60 - 110	1.4	70 – 124	3.6	190 – 230	4.1
110 - 160	2.3	124 - 201	1.2	230 - 280	3.5
160 – 230	3.4	201 – 270	4.1	280 – 320	2.2
>230	1.2	>270	2.8	>320	0.5

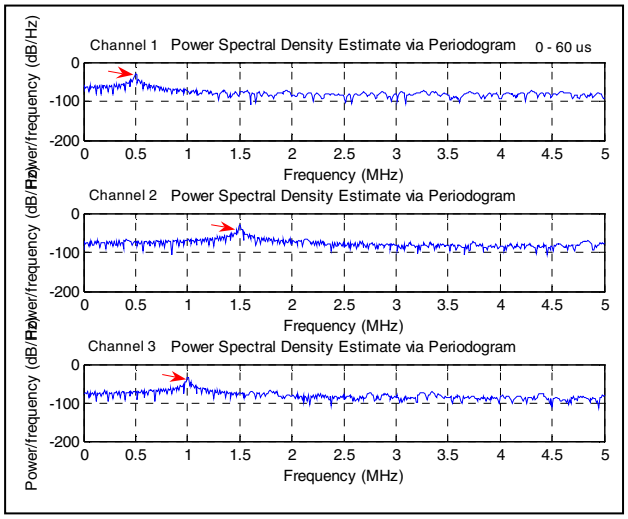

Fig. 4 Output of MOSAICS after filtering for IF signals (0 – 60 μs).

sampling scheme [2], $R_{OP} = 10\,MHz$. The Power Spectral Density (PSD) estimate (Table 2B) of the three MOSAICS outputs is found after passing through a 20 tap low pass (0-5 MHz) filter. It is clear from the table that the frequencies of the maximum PSD values in all time intervals perfectly match with that expected due to translation of the spectrum on account of band pass sampling at 10 MHz followed by low pass filtering. A snapshot of the PSD output in the interval 0-60 μs is shown in Fig. 4. The peaks are indicated by red arrows. This suggests that MOSAICS is well suited in applications where exact recovery of the signal after sampling is not so much important as the mere detection of the prominent Doppler frequency bin.

VII. CONCLUSIONS

Multiple analog signals which exhibit local spectral sparsity can be acquired with a limited set of measurements and reconstructed in a compressed sensing framework under the MOSAICS scheme that we have proposed in this paper. The MOSAICS setup employs a single, uniform rate ADC, which optimally samples data from several analog channels with the help of an analog multiplexer. We envisage that the multiplexed acquisition scheme proposed can employ any other arbitrary sampling strategy also. We have also presented a hardware implementation, based on easily available computer electronics, for MOSAICS. We have also conveyed the results on two test signals in the presence of simulated measurement noise, demonstrating very high reconstruction accuracy.

REFERENCES

[1] H. J. Landau, "Necessary density conditions for sampling and interpolation of certain entire functions," *Acta Math.*, vol. 117, pp. 37–52, Feb. 1967.

[2] R. G. Vaughan, N. L. Scott, and D. R. White, "The theory of bandpass sampling," *IEEE Trans. Signal Process.*, vol. 39, no. 9, pp. 1973–1984, Sep. 1991.

[3] Kohlenberg, "Exact interpolation of band-limited functions," J. *Appl. Phys.*, vol. 24, pp. 1432–1435, Dec. 1953.

[4] Y.-P. Lin and P. P. Vaidyanathan, "Periodically nonuniform sampling of bandpass signals," *IEEE Trans. Circuits Syst. II*, vol. 45, no. 3, pp. 340–351, Mar. 1998.

[5] P. Feng and Y. Bresler, "Spectrum-blind minimum-rate sampling and reconstruction of multiband signals," in *Proc. IEEE Int. Conf. Acoustics, Speech, Signal Processing (ICASSP)*, May 1996, vol. 3, pp. 1688–1691.

[6] Y. Bresler and P. Feng, "Spectrum-blind minimum-rate sampling and reconstruction of 2-d multiband signals," in *Proc. IEEE Int. Conf. Image Process.*, Sep. 1996, vol. 1, pp. 701–704.

[7] R. Venkataramani and Y. Bresler, "Further results on spectrum blind sampling of 2D signals," in *Proc. IEEE Int. Conf. Image Process.*, Oct. 4–7, 1998, vol. 2, pp. 752–756.

[8] R. Venkataramani and Y. Bresler, "Perfect reconstruction formulas and bounds on aliasing error in sub-Nyquist nonuniform sampling of multiband signals," *IEEE Trans. Inf. Theory*, vol. 46, no. 6, pp. 2173–2183, Sep. 2000.

[9] Moshe Mishali and Yonina C. Eldar, "Blind Multiband Signal Reconstruction: Compressed Sensing for Analog Signals", *IEEE Trans. Sig. Proc*, vol. 57, no. 4, pp. 993 – 1009, Mar. 2009.

[10] J. A. Tropp, J.N. Laska, M. F. Duarte, J.K. Romberg and R. G. Baraniuk, "Beyond Nyquist: Efficient sampling of sparse bandlimited signals," *IEEE Trans. Info. Theory*, vol. 56, no. 1, pp. 520 – 544, Jan 2010.

[11] T. Ragheb, S. Kirolos,, J. Laska, ,A. Gilbert, M. Strauss, R. Baraniuk and Y. Massoud, "Implementation models for analog-to-information conversion via random sampling", Midwest symposium on Circuits and Systems, 2007

[12] D.L. Donoho, "Compressed Sensing", IEEE Trans. Inform. Theory, vol. 52, no. 4, pp. 1289–1306, Apr. 2006.

[13] E. Candes and M. Wakin, "An introduction to compressive sampling," IEEE Signal Proc. Magazine, vol. 25, no. 2, pp. 21–30, March 2008.

[14] E. Cand`es, J. Romberg, and T. Tao, "Robust uncertainty principles: Exact signal reconstruction from highly incomplete frequency information," IEEE Trans. Inform. Theory, vol. 52, no. 2, pp. 489–509, Feb. 2006.

[15] E. Candes and J. Romberg, "Sparsity and incoherence in compressive sampling," *Inverse Problems*, vol. 23, pp. 969–985, April 2007.

[16] S.S. Chen, D.L. Donoho, and M.A. Saunders, "Atomic decomposition by basis pursuit," SIAM J. Sci. Comput., vol 20, no 1, pp 33–61, 1999.

[17] E. Candes and T.Tao, "Near Optimal Signal Recovery from Random projections: Universal encoding strategies", IEEE Trans. Inform. Theory, vol. 52, no. 12, pp. 5406–5425, Dec.. 2006.

[18] E. Candès and J. Romberg, 2005. "Practical signal recovery from random projections," in Proc. SPIE Int. Symp. Electron. Imag., pp.76–86.

[19] M. I. Skolnik, "Introduction to Radar Systems", McGraw Hill 1981

[20] S.M. Sherman, "Monopulse Principles and Techniques", Artech House Inc., 1984